

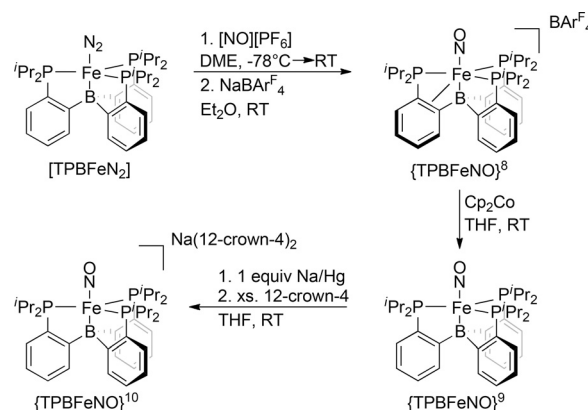
## Iron Nitrosyl Complexes

International Edition: DOI: 10.1002/anie.201605403  
German Edition: DOI: 10.1002/ange.201605403A Triad of Highly Reduced, Linear Iron Nitrosyl Complexes:  $\{\text{FeNO}\}^{8-10}$ 

Matthew J. Chalkley and Jonas C. Peters\*

**Abstract:** Given the importance of Fe–NO complexes in both human biology and the global nitrogen cycle, there has been interest in understanding their diverse electronic structures. Herein a redox series of isolable iron nitrosyl complexes stabilized by a tris(phosphine)borane (TPB) ligand is described. These structurally characterized iron nitrosyl complexes reside in the following highly reduced Enemark–Feltham numbers:  $\{\text{FeNO}\}^8$ ,  $\{\text{FeNO}\}^9$ , and  $\{\text{FeNO}\}^{10}$ . These  $\{\text{FeNO}\}^{8-10}$  compounds are each low-spin, and feature linear yet strongly activated nitric oxide ligands. Use of Mössbauer, EPR, NMR, UV/Vis, and IR spectroscopy, in conjunction with DFT calculations, provides insight into the electronic structures of this uncommon redox series of iron nitrosyl complexes. In particular, the data collectively suggest that  $\{\text{TPBFeNO}\}^{8-10}$  are all remarkably covalent. This covalency is likely responsible for the stability of this system across three highly reduced redox states that correlate with unusually high Enemark–Feltham numbers.

Due to the prevalence of both heme and non-heme iron nitrosyl units in biology,<sup>[1]</sup> iron model complexes bearing nitrosyl ligands have been the subject of study for decades.<sup>[2]</sup> Many examples of  $\{\text{FeNO}\}^6$  and  $\{\text{FeNO}\}^7$  complexes are known<sup>[3]</sup> and, more recently, several  $\{\text{FeNO}\}^8$  complexes have been thoroughly characterized.<sup>[4,5]</sup> However,  $\{\text{FeNO}\}^9$  complexes are unknown, and the unique properties of the only known example of an  $\{\text{FeNO}\}^{10}$  complex,  $[\text{Fe}(\text{CO})_3\text{NO}]^-$ , prompted its reinvestigation in 2014 by Plietker and co-workers.<sup>[6]</sup> The unusually low wavenumber found for the stretching vibration of the NO ligand ( $\tilde{\nu} = 1647\text{ cm}^{-1}$ ) and long N–O bond ( $1.212\text{ Å}$ ) but linear Fe–N–O angle ( $180^\circ$ ) observed in this latter complex stand in contrast to the literature on iron nitrosyl complexes, where strong activation of the coordinated NO unit leads to a bent geometry.<sup>[4]</sup> Therefore, we sought to investigate the Fe–NO unit under local threefold symmetry on a ligand platform that would engender strong Fe–N multiple bonding while also providing redox flexibility. With this in mind, we pursued the synthesis of a series of Fe–NO complexes supported by a tris(phosphine)borane (TPB) ligand (Scheme 1).<sup>[7]</sup> Herein we report the synthesis of a monoiron mononitrosyl complex that has

Scheme 1. Synthesis of  $\{\text{TPBFeNO}\}^{8-10}$ .

been crystallographically characterized across three oxidation states, including highly unusual examples of  $\{\text{FeNO}\}^9$  and  $\{\text{FeNO}\}^{10}$  complexes. These nitrosyl complexes are distinct in their retention of a strictly linear Fe–N–O unit across the series; a high degree of covalency facilitates this atypical structural behavior.<sup>[8]</sup>

In our exploration of Fe–N<sub>2</sub> chemistry, the TPB ligand has demonstrated the ability to support strong Fe–N  $\pi$  bonding, while geometric (and electronic) flexibility of the Fe–B interaction allows for stabilization of highly reduced Fe species. Given that  $[\text{TPBFeN}_2]$  has an irreversible oxidation event that causes dissociation of the N<sub>2</sub> ligand to generate  $[\text{TPBFe}]^+$ , we hypothesized that nitrosonium hexafluorophosphate ( $[\text{NO}][\text{PF}_6]$ ) could serve both to oxidize  $[\text{TPBFeN}_2]$  and to act as a source of in situ nitric oxide to bind Fe.<sup>[9]</sup> Isolation of the  $\{\text{TPBFeNO}\}^8$  cation as its  $\text{BARF}_4$  salt (after salt metathesis with  $\text{NaBARF}_4$ ;  $\text{BARF}_4 = \text{B}-(3,5-(\text{CF}_3)_2\text{C}_6\text{H}_3)_4$ ) proved viable (Scheme 1). The cyclic voltammetry of  $\{\text{TPBFeNO}\}^8$  (see Supporting Information, Figure S30) demonstrated both a quasi-reversible reduction at  $-0.56\text{ V vs. Fc/Fc}^+$  and a second, fully reversible feature at  $-1.97\text{ V vs. Fc/Fc}^+$ . We attribute these redox features to the  $\{\text{FeNO}\}^{8/9}$  and  $\{\text{FeNO}\}^{9/10}$  couples, respectively. Synthetic generation of neutral  $\{\text{TPBFeNO}\}^9$  via cobaltocene reduction of  $\{\text{TPBFeNO}\}^8$ , and anionic  $\{\text{TPBFeNO}\}^{10}$  via Na/Hg reduction of  $\{\text{TPBFeNO}\}^9$ , provided the desired  $\{\text{TPBFeNO}\}^{8-10}$  series (Scheme 1). In contrast to most other reports of highly reduced Fe–NO complexes,<sup>[4,13b]</sup> these three species are stable both in solution and in the solid state at room temperature under an inert atmosphere.

The infrared spectra of  $\{\text{TPBFeNO}\}^{8-10}$  demonstrate an approximately  $\Delta\tilde{\nu} = 100\text{ cm}^{-1}$  decrease in the wavenumber of the stretching frequency of the N–O ligand upon each successive reduction (Figure 1). This behavior is reminiscent

\* M. J. Chalkley, Prof. Dr. J. C. Peters  
Division of Chemistry and Chemical Engineering  
California Institute of Technology  
1200 E. California Blvd., Pasadena, CA 91125 (USA)  
E-mail: jpeters@caltech.edu

Supporting information and the ORCID identification number(s) for the author(s) of this article can be found under <http://dx.doi.org/10.1002/anie.201605403>.

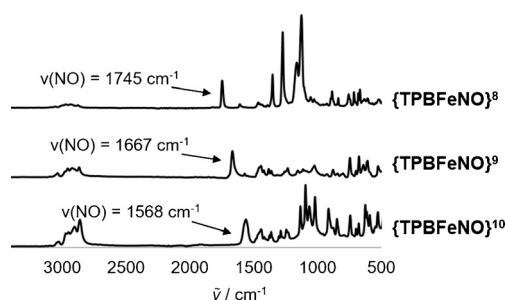


**Figure 1.** Thin-film IR spectra of  $\{\text{TPBFeNO}\}^{8-10}$  highlighting the frequencies of their NO stretching vibrations.

of that seen in transition-metal complexes of  $\pi$ -accepting ligands such as  $\text{N}_2$  and  $\text{CO}$ .<sup>[9,10]</sup> However, it stands in contrast to that of most previously characterized iron nitrosyl complexes, which more typically show much larger changes ( $\Delta\tilde{\nu} = 200\text{--}350\text{ cm}^{-1}$ ) in the NO stretching vibration per unit change in their Enemark–Feltham number.<sup>[4a,f]</sup> This observation suggested to us that the Fe–NO linkage remains linear throughout the redox series described here, a behavior that is rare in redox series of metal nitrosyl complexes.<sup>[3]</sup> The crystal structures of  $\{\text{TPBFeNO}\}^{8-10}$  confirm that the Fe–N–O angle is highly linear in each complex:  $175.8(3)^\circ$  in  $\{\text{TPBFeNO}\}^8$ ,  $176.18(6)^\circ$  in  $\{\text{TPBFeNO}\}^9$ , and  $179.05(12)^\circ$  in  $\{\text{TPBFeNO}\}^{10}$ .

The crystal structures<sup>[11]</sup> (Figure 2) of  $\{\text{TPBFeNO}\}^{8-10}$  further reveal that the only significant ligand rearrangement across the series is the presence of an intramolecular  $\eta^4$ -BCCP interaction in  $\{\text{TPBFeNO}\}^8$ . Variable-temperature  $^1\text{H}$  and  $^{31}\text{P}$  NMR experiments indicate that this interaction is maintained in solution (Figure S1–S4). In contrast, both  $\{\text{TPBFeNO}\}^9$  and  $\{\text{TPBFeNO}\}^{10}$  demonstrate approximate threefold symmetry in solution as well as in the solid state. Although Fe–N–O linearity is maintained, the N–O bond does lengthen about  $0.03\text{ \AA}$  upon each reduction, in agreement with the activation observed by IR spectroscopy. Although the Fe–N bond distance remains fairly constant (Table S3), the Wiberg bond indices (Table S27) show that the Fe–N bond order increases slightly from  $\{\text{TPBFeNO}\}^8$  to  $\{\text{TPBFeNO}\}^{10}$  with a concomitant decrease in the N–O bond order.<sup>[12]</sup> In addition to Fe–N bonding, the Wiberg bond index shows significant Fe–O bonding (bond order of ca. 0.5). This through-atom interaction has been previously interpreted as indicative of a highly covalent interaction.<sup>[12a]</sup> Although the Fe–B bond length increases with reduction, possibly suggestive of a weakening Fe–B interaction, the boron does become more pyramidalized, which agrees with both the DFT calculations (see below) and the  $^{11}\text{B}$  NMR spectra (Figures S5 and S12), and suggests increased Fe–B bonding upon reduction. Finally, the Fe–P distances are significantly shorter in  $\{\text{TPBFeNO}\}^{10}$  than in both  $\{\text{TPBFeNO}\}^8$  and  $\{\text{TPBFeNO}\}^9$ , likely due to increased Fe–P backbonding in the most reduced species.

Mössbauer spectroscopy has been frequently employed in the study of iron nitrosyl complexes as an experimental probe of the relative state of oxidation of the iron center.<sup>[4a,f,6b,8,13]</sup> Typically, octahedral  $\{\text{FeNO}\}^6$  complexes have isomer shifts between  $0.0$  and  $0.05\text{ mm s}^{-1}$ ,  $\{\text{FeNO}\}^7$  complexes have isomer shifts between  $0.25$  and  $0.33\text{ mm s}^{-1}$ , and  $\{\text{FeNO}\}^8$  complexes

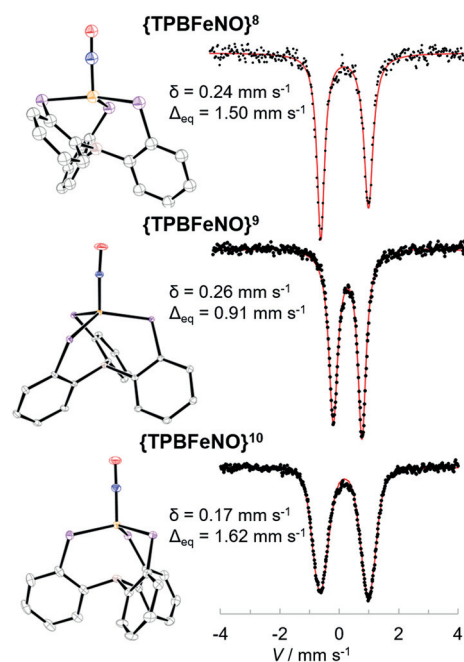


**Figure 2.** Left: X-ray crystal structures of  $\{\text{TPBFeNO}\}^{8-10}$ . Thermal ellipsoids are set at 50% probability. Isopropyl groups, hydrogen atoms, solvent molecules, and counterions are omitted for clarity. Fe orange, P pink, N blue, O red, B brown, C gray. Right: Zero-field, 80 K Mössbauer spectra for samples of microcrystalline  $\{\text{TPBFeNO}\}^{8-10}$  suspended in a boron nitride matrix. Data are shown as black dots and the fit is shown as a red line. Fit parameters are as shown; linewidths can be found in the Supporting Information along with additional spectra.<sup>[14]</sup>

have isomer shifts between  $0.4$  and  $0.5\text{ mm s}^{-1}$ . These significant changes in the isomer shift occur despite NO-centered reduction due to the decreasing ability of the NO ligand to accept electron density through backbonding.<sup>[4a]</sup> For the high-spin, pseudo- $\text{C}_3$   $\{\text{FeNO}\}^{6-8}$  recently reported by Lehnert et al., even larger changes in isomer shift (ca.  $0.4\text{ mm s}^{-1}$ ) per unit reduction are observed. These authors suggest that such a large shift is indicative of metal-centered reduction.<sup>[13a]</sup>

The zero-field, 80 K Mössbauer spectra of  $\{\text{TPBFeNO}\}^{8-10}$  (Figure 2) show only very minimal changes in the isomer shift as a function of the overall redox state. The linear and therefore strongly  $\pi$ -bound NO ligand enforces low-spin configurations for all three redox states, leading to short metal–ligand bonds and correspondingly low isomer shifts.<sup>[15]</sup> These low isomer shifts are consistent with the behavior observed in other highly-reduced TPBFe complexes, related tris(phosphine)silyl-supported Fe complexes, and a very recently reported series of linear  $\{\text{FeNO}\}^{6-8}$  in tetragonal symmetry.<sup>[8,16]</sup> Even within this context, the  $\{\text{TPBFeNO}\}$  system is remarkable for the minimal change in isomer shift observed across the redox series; this suggests a high degree of metal–ligand covalency that buffers against any buildup of electron density on the iron center upon successive reductions.<sup>[17]</sup>

The electronic structures of metal nitrosyl complexes are still debated,<sup>[18]</sup> but linear NO complexes are most commonly described by a  $\pi$ -accepting  $\text{NO}^+$  resonance form. In Fe–

(NO<sup>+</sup>) complexes, the NO stretching vibration is typically found between  $\tilde{\nu}=1900$  and  $2000\text{ cm}^{-1}$ .<sup>[19]</sup> There are also cases where a linear nitrosyl unit is considered to be a  $\pi$ -donating NO<sup>-</sup> ligand.<sup>[4e,6b]</sup> These two limiting resonance forms indicate formal charge transfer either from the NO to the metal center or from the metal center to the NO. To help determine which, if either, of these limiting cases more accurately describes the complexes featured herein, we draw comparisons to the known dinitrogen (N<sub>2</sub> is isolobal to NO<sup>+</sup>) and imido (NR is isolobal to NO<sup>-</sup>) complexes of the TPBFe scaffold.<sup>[8,16b]</sup> Relative to the {TPBFeNO} complexes, the TPBFeN<sub>2</sub> complexes have longer Fe–N (ca. 1.78 Å) distances and shorter Fe–B distances (ca. 1.3 Å), suggesting a weaker  $\pi$  interaction between the Fe atom and the N<sub>2</sub> ligand and more  $\sigma$  backdonation into the borane.<sup>[20]</sup> In contrast, the TPBFe(NR) complexes have similarly short Fe–N (1.66 Å) distances but much longer Fe–B (2.6–2.8 Å) distances, arising from a distortion to a more tetrahedral symmetry at the iron center that further enhances Fe–N  $\pi$  bonding, and a more electron poor Fe center with minimal backdonation into the borane.<sup>[21]</sup> It therefore seems apparent that neither limiting scenario (Fe–(NO<sup>+</sup>) vs. Fe–(NO<sup>-</sup>)) reliably describes the bonding situation observed in the {TPBFeNO}<sup>8–10</sup> series. A description of the entire ligand sphere about the iron center as covalent seems more appropriate than descriptions that imply significant charge transfer.

This covalent description is further supported by the cryogenic-temperature (–180 °C) UV/Vis spectrum of {TPBFeNO}<sup>9</sup> (Figure 3). Upon cooling, a vibronic progression with spacing of 452, 457, 476, 509, 499 cm<sup>-1</sup> emerges on the electronic transition centered at  $\lambda=521\text{ nm}$ . To our knowledge, a related vibronic progression has been observed in only one other M–NO system, characterized by Gray and co-workers in 1966 in the cryogenic electronic spectrum of [Cr(CN)<sub>5</sub>NO]<sup>3-</sup>. In that case, the electronic transition featuring the vibronic progression was centered at  $\lambda=470\text{ nm}$  and was attributed to a transition from a metal-based d<sub>xy</sub> or d<sub>x<sup>2</sup>-y<sup>2</sup></sub> orbital into a Cr–N  $\pi^*$  orbital. Although this previous study investigated a series of isoelectronic, pentacyano metal (M = V, Cr, Mn, Fe) nitrosyl complexes, only [Cr(CN)<sub>5</sub>NO]<sup>3-</sup> revealed vibronic progression upon cooling. The orbital

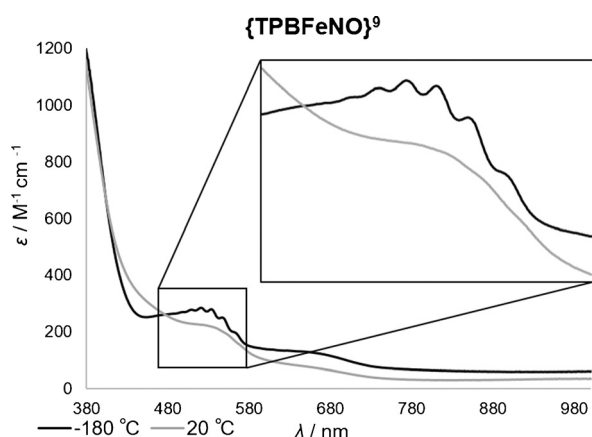


**Figure 3.** Density-corrected<sup>[22]</sup> room temperature (solution) and cryogenic (frozen glass) UV/Vis spectra of {TPBFeNO}<sup>9</sup> in 2-MeTHF highlighting the region that demonstrates vibronic progression.

contribution from Cr and NO  $\pi^*$  to the Cr–N  $\pi^*$  orbital was deduced to be nearly equal, leading the authors to posit that this might be requisite for the observation of vibronic progression.<sup>[23]</sup> Likewise, cooling of {TPBFeNO}<sup>8</sup> and {TPBFeNO}<sup>10</sup>, which exhibit absorption features at a similar wavelength, does not lead to the emergence of a vibronic progression (Figures S17 and S18). Due to the similarities in M–N–O angle, N–O distance, and  $\nu(\text{NO})$  (Table S1) of [Cr(CN)<sub>5</sub>NO]<sup>3-</sup> and {TPBFeNO}<sup>9</sup>, and the observation that the calculated d<sub>xy</sub>–Fe–N  $\pi^*$  gap (SOMO–LUMO gap) in {TPBFeNO}<sup>9</sup> is  $\lambda=520\text{ nm}$ , we also assign this absorption feature to a d<sub>xy</sub>–M–N  $\pi^*$  transition.<sup>[24]</sup> Based on our own observations, those of Gray and co-workers, and the paucity of metal–NO complexes demonstrating such vibronic progression, it appears that vibronic progression of this type is only (albeit not necessarily) observed in highly covalent, linear M–NO units.

The solution magnetic susceptibility of {TPBFeNO}<sup>9</sup> is  $1.7\mu_{\text{B}}$  (C<sub>6</sub>D<sub>6</sub>, room temperature), consistent with an  $S=1/2$  species. The X-band EPR spectrum of {TPBFeNO}<sup>9</sup> (Figure S34) shows a nearly axial signal with significant  $g$  anisotropy and broad features. We favor an electronic structure consistent with a description in which the SOMO consists of an iron d orbital that is primarily of d<sub>xy</sub> or d<sub>x<sup>2</sup>-y<sup>2</sup></sub> parentage, akin to ferrocenium.<sup>[25]</sup> Unrestricted DFT calculations using BP86/def2-TZVVP (Fe, B, P, N, O) and 631-G(d) (C, H)<sup>[26]</sup> reproduce the structure of {TPBFeNO}<sup>9</sup> well and support this description (Figure 4).<sup>[27]</sup>

The collective data presented here lend support to an electronic description of {TPBFeNO}<sup>8–10</sup> in which reduction of the system across the Enemark–Feltham numbers from 8 to 9 and 9 to 10 occurs in primarily Fe-based orbitals that are orthogonal to both the Fe–NO  $\pi$  bonds and the Fe–B  $\sigma$  bond. However, as the Fe becomes more electron-rich, backbonding into the NO,  $\sigma$  backbonding into the borane, and presumably  $\pi$  backbonding into the phosphines all become stronger

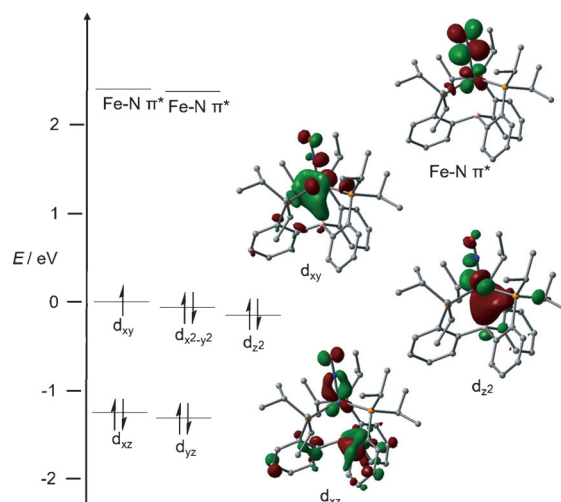


**Figure 4.** A molecular orbital diagram for {TPBFeNO}<sup>9</sup>. The energies given are relative to the SOMO which was set to be 0 eV. The molecular orbitals depicted (isovalue = 0.05) are from the  $\alpha$ -spin manifold as are the energies. The energy and appearance of the  $\beta$ -spin orbitals are similar (Figure S58).



leading to very little overall change in the electron density at the Fe center (i.e. its relative state of oxidation).

This high degree of covalency, particularly in the Fe–NO bond but also between the Fe and the TPB ligand, leads to the atypical maintenance of a linear Fe–N–O geometry upon successive reductions and appears to be key to the ability of the TPB ligand to support an Fe–NO unit across three redox states. Finally, trigonal symmetry, rather than tetragonal symmetry, gives rise to an additional non-bonding orbital, providing access to unusually high Enemark–Feltham numbers (8, 9, and 10).

## Acknowledgements

This research was supported by the NIH (GM-070757) and an NSF Graduate Research Fellowship to M.J.C. We thank Larry Henling and Dr. Michael K. Takase for crystallographic assistance. We acknowledge Dr. Gaël Ung for preliminary data on the  $\{TPBFeNO\}^8$  complex and helpful discussions.

**Keywords:** boratrane · coordination modes · iron · metal–ligand covalency · nitrogen oxides

**How to cite:** *Angew. Chem. Int. Ed.* **2016**, 55, 11995–11998  
*Angew. Chem.* **2016**, 128, 12174–12177

- [1] a) P. Pacher, J. S. Beckman, L. Liaudet, *Physiol. Rev.* **2007**, 87, 315; b) A. G. Tennyson, S. J. Lippard, *Chem. Biol.* **2011**, 18, 1211.
- [2] J. H. Enemark, R. D. Feltham, *Coord. Chem. Rev.* **1974**, 13, 339.
- [3] a) T. W. Hayton, P. Legzdins, W. B. Sharp, *Chem. Rev.* **2002**, 102, 935; b) A. M. Wright, T. W. Hayton, *Comments Inorg. Chem.* **2012**, 33, 207.
- [4] a) R. G. Serres, C. A. Grapperhaus, E. Bothe, E. Bill, T. Weyhermüller, F. Neese, K. Wieghardt, *J. Am. Chem. Soc.* **2004**, 126, 5138; b) J. Pellegrino, S. E. Bari, D. E. Bikiel, F. Doctorovich, *J. Am. Chem. Soc.* **2010**, 132, 989; c) B. C. Sanders, A. K. Patra, T. C. Harrop, *J. Inorg. Biochem.* **2013**, 118, 115; d) L. E. Goodrich, S. Roy, E. E. Alp, J. Zhao, M. Y. Hu, N. Lehnert, *Inorg. Chem.* **2013**, 52, 7766; e) A. L. Speelman, N. Lehnert, *Angew. Chem. Int. Ed.* **2013**, 52, 12283; *Angew. Chem.* **2013**, 125, 12509; f) B. Hu, J. Li, *Angew. Chem. Int. Ed.* **2015**, 54, 10579; *Angew. Chem.* **2015**, 127, 10725.
- [5] Enemark–Feltham notation is widely used in metal nitrosyl chemistry and is determined by summing the number of metal d electrons and N–O  $\pi^*$  electrons.
- [6] a) W. Hieber, K. Beutner, *Z. Naturforsch. B* **1960**, 15, 323; b) J. E. Klein, B. Miehl, M. S. Holzwarth, M. Bauer, M. Milek, M. M. Khusniyarov, G. Knizia, H. J. Werner, B. Plietker, *Angew. Chem. Int. Ed.* **2014**, 53, 1790; *Angew. Chem.* **2014**, 126, 1820.
- [7] S. Bontemps, G. Bouhadir, K. Miqueu, D. Bourissou, *Inorg. Chem.* **2007**, 46, 5149.
- [8] During the preparation of this manuscript for submission, a publication featuring a crystallographically characterized redox series of  $\{FeNO\}^{6-8}$  featuring linear Fe–N–O angles in tetragonal symmetry appeared online: C. Kupper, J. A. Rees, S. Dechert, S. DeBeer, F. Meyer, *J. Am. Chem. Soc.* **2016**, 138, 7888.
- [9] M.-E. Moret, J. C. Peters, *Angew. Chem. Int. Ed.* **2011**, 50, 2063; *Angew. Chem.* **2011**, 123, 2111.
- [10] Y. Lee, J. C. Peters, *J. Am. Chem. Soc.* **2011**, 133, 4483.
- [11] CCDC 1481636 ( $\{TPBFeNO\}^8$ ), 1481637 ( $\{TPBFeNO\}^9$ ), and 1481638 ( $\{TPBFeNO\}^{10}$ ) contain the supplementary crystallographic data for this paper. These data can be obtained free of charge from The Cambridge Crystallographic Data Centre.
- [12] a) O. V. Sizova, A. Y. Sokolov, L. V. Skripnikov, V. I. Baranovskii, *Polyhedron* **2007**, 26, 4680; b) M.-E. Moret, J. C. Peters, *J. Am. Chem. Soc.* **2011**, 133, 18118.
- [13] a) A. L. Speelman, B. Zhang, C. Krebs, N. Lehnert, *Angew. Chem. Int. Ed.* **2016**, 55, 6685; *Angew. Chem.* **2016**, 128, 6797; b) A. K. Patra, K. S. Dube, B. C. Sanders, G. C. Papaefthymiou, J. Conradie, A. Ghosh, T. C. Harrop, *Chem. Sci.* **2012**, 3, 364; c) Y. Zhang, E. Oldfield, *J. Am. Chem. Soc.* **2004**, 126, 9494.
- [14] Asymmetric quadrupole doublets in diamagnetic species can be caused by a variety of solid-state effects. We believe that to be the case here as both powdered samples and  $^{57}Fe$ -enriched 2-MeTHF solution samples demonstrate symmetric quadrupole doublets. (See Mössbauer section of the Supporting Information for a further discussion and additional spectra.)
- [15] a) P. Gülich, E. Bill, A. X. Trautwein *Mössbauer Spectroscopy and Transition Metal Chemistry: Fundamentals and Applications*, Springer, Heidelberg, **2011**, pp. 72–137; b) S. Ye, E. Bill, F. Neese, *Inorg. Chem.* **2016**, 55, 3468.
- [16] a) Y. Lee, N. P. Mankad, J. C. Peters, *Nat. Chem.* **2010**, 2, 558; b) J. S. Anderson, G. E. Cutsail III, J. Rittle, B. A. Connor, W. A. Gunderson, L. Zhang, B. M. Hoffman, J. C. Peters, *J. Am. Chem. Soc.* **2015**, 137, 7803; c) T. J. Del Castillo, N. B. Thompson, J. C. Peters, *J. Am. Chem. Soc.* **2016**, 138, 5341.
- [17] As we noted in Ref. [16c], strong covalency between the metal and the TPB ligand leads to a non-classical relationship between isomer shift and redox state in these species. Low-spin complexes of these types feature low isomer shifts regardless of formal oxidation state.
- [18] N. C. Tomson, M. R. Crimmin, T. Petrenko, L. E. Rosebrugh, S. Sproules, W. C. Boyd, R. G. Bergman, S. DeBeer, F. D. Toste, K. Wieghardt, *J. Am. Chem. Soc.* **2011**, 133, 18785.
- [19] H. Lewandowska, *Nitrosyl Complexes in Inorganic Chemistry, Biochemistry and Medicine I* (Ed.: D. M. P. Mingos), Springer, Heidelberg, **2014**, pp. 45–167.
- [20] For comparison, the Wiberg bond index calculation for  $[TPBFeN_2]^-$  (isoelectronic to  $[TPBFeNO]^9$ ) provides an Fe–B bond order of 0.5526 compared to 0.4402 and an Fe–N bond order of 0.9796 compared to 1.5958.
- [21] For comparison, the Wiberg bond index calculation for  $[TPBFe(NA)]^+$  (isoelectronic to  $[TPBFeNO]^9$ ) provides an Fe–B bond order of 0.2718 compared to 0.4402 and an Fe–N bond order of 1.7980 compared to 1.5958.
- [22] K. Shinsaka, N. Gee, G. R. Freeman, *J. Chem. Thermodyn.* **1985**, 17, 1111.
- [23] P. T. Manoharan, H. B. Gray, *Inorg. Chem.* **1966**, 5, 823.
- [24] J. H. Enemark, M. S. Quinby, L. R. Reed, M. J. Steuck, K. K. Walther, *Inorg. Chem.* **1970**, 9, 2397.
- [25] Y. S. Sohn, D. N. Hendrickson, H. B. Gray, *J. Am. Chem. Soc.* **1970**, 92, 3233.
- [26] a) W. J. Hehre, R. Ditchfield, J. A. Pople, *J. Chem. Phys.* **1972**, 56, 2257; b) J. P. Perdew, *Phys. Rev. B* **1986**, 33, 8822; c) A. D. Becke, *Phys. Rev. A* **1988**, 38, 3098; d) A. Schaefer, H. Horn, R. Ahlrichs, *J. Chem. Phys.* **1992**, 97, 2571; e) F. Weigend, R. Ahlrichs, *Phys. Chem. Chem. Phys.* **2005**, 7, 3297.
- [27] Broken-symmetry calculations, in which an  $S=1$   $NO^-$  is anti-ferromagnetically coupled to a metal center, are often used in the case of linear M–NO complexes. Attempts to optimize such wavefunctions with BP86 led to their collapse back to the low-spin wavefunction. Further DFT discussions including low-spin and broken-symmetry calculations with B3LYP can be found in the Supporting Information.

Received: June 2, 2016

Revised: July 10, 2016

Published online: August 25, 2016